Numerical simulation of DA white dwarf surface convection

Numerical simulation of DA white dwarf surface convection

[1]F. Zaussinger, [2]F. Kupka, [3]M. Montgomery, [1]Ch. Egbers

[1] BTU Cottbus-Senftenberg, Departement for Aerodynamics and Fluid Mechanics, Cottbus, Germany

[2] Institute for Astrophysics, University of Göttingen, Friedrich-Hund-Platz 1, 37077 Göttingen, Germany

[3] Department of Astronomy and McDonald Observatory, University of Texas at Austin, Austin, TX, 78712, USA

E-mail: `florian.zaussinger@b-tu.de`

Abstract. White dwarfs are compact objects with masses comparable to our Sun, but a radius similar to our Earth. They are the final evolutionary stage for about 95% of all stars in the Galaxy, i.e., for all stars that have a final mass less than the Chandrasekhar mass (about 1.4 times the solar mass), the upper mass limit for which hydrostatic equilibrium can be maintained by the degeneracy pressure of electrons at very high densities. The outermost shell of most white dwarfs contains a convective layer. Even if the latter is very thin ($\lesssim 10\,\mathrm{km}$), it is important for mixing properties, observed radiation, and pulsational stability of the whole object. During a long phase white dwarfs have effective temperatures T_{eff} of about $10000\,\mathrm{K} \sim 14000\,\mathrm{K}$, since the time scale to reach such temperatures by cooling is already $\approx 10^9$ years. Here, we focus on DA (hydrogen-rich) white dwarfs with $T_{\mathrm{eff}} \approx 12000\,\mathrm{K}$. This is at the transition from shallow to deep convection zones. Due to very high gravitational acceleration ($\sim 10^6$ g at the surface) the material is overturned about five times per second over the distance of a few kilometers. Numerical simulations of such objects have to be done for a compressible flow and feature highly turbulent granules at the surface, which are qualitatively comparable to the convection cells observed at the surface of the Sun. For this study we compare three white dwarf surface simulations with realistic microphysical properties and full 3D radiative transport. The simulations differ in effective temperature, namely, $T_{\mathrm{eff}} = 11800\,\mathrm{K}$, $12100\,\mathrm{K}$, and $12400\,\mathrm{K}$. A statistical analysis of the convective processes as function of T_{eff} is presented.

1. Introduction

About 20 years ago a first effort in performing numerical hydrodynamical simulations of the surface layers of DA type white dwarfs was made, [1]. It had to be limited to just two spatial dimensions and rather low numerical resolution, with typically less than 100 grid points per direction. After having constructed a new code (CO5BOLD, for a review see [2]), the same group performed numerical hydrodynamical simulations for these objects in three spatial dimensions, [11]. With a resolution of 150 grid points per direction these simulations aimed at constructing a grid of models as a function of effective temperature T_{eff} and surface gravity to investigate problems of observational spectroscopy, [11, 12]. More recently, these simulations have also been used to investigate the physics of overshooting underneath the convection zone and calibrate simple convection models and estimates of convection induced mixing, [10]. The

present numerical simulations differ from previous work, among others, in the following aspects. First of all, ANTARES [9, 13, 4] has a much lower intrinsic numerical viscosity (fifth order WENO) than the numerical schemes used in actual runs with CO5BOLD (typically second order with shock and subgrid scale viscosity). Secondly, we suggest simulations to be performed which cover a much deeper and wider domain with typically around 400 grid points per direction. Together these two features should allow a more accurate quantification of convective mixing and convective overshooting and more reliable statistical analyses. Thirdly, the grid refinement capability of ANTARES optionally allows a fully turbulent flow simulation for limited areas of the simulation domain. Previous work had to remain limited to simulations of a laminar flow at the grid scale with turbulence represented only through subgrid scale modelling, [6]. Finally, since ANTARES is parallelized according to the MPI paradigm (and some parts in a hybrid parallelization based on both MPI and OpenMP), much larger simulations on supercomputers based on more varied hardware are possible compared to a code parallelized through OpenMP only. Thus, ANTARES is ideally suited for the specific challenges posed by the numerical simulations on super computer clusters required to be done to gain further insight into the physics of overshooting and mixing in DA white dwarf stars.

1.1. Settling of heavy elements and overshooting

Due to their high surface gravities diffusion of elements in the upper part of white dwarf envelopes occurs on short time scales. DA white dwarfs have a residual amount of hydrogen which after a phase of gravitational settling "floats" on top of fluid consisting of heavier elements (helium around a core chiefly made of carbon and oxygen). Hence, their atmospheres consist of nearly pure hydrogen. Indeed, for a non-convective atmosphere calculations show that heavy elements like Ca or Mg should settle out of the photosphere in one or two weeks. This is important because actually Ca and Mg are observed in the photospheres of up to 25% of all DA WDs [3, 5]. It has been suggested that these elements are continuously accreted. To calculate accretion rates the settling rates have to be known in turn. This is straightforward to do if the star is not convective, but if there is a surface convection zone, the relevant settling rate is the rate at the base of the convection zone. Since the important physical process in this context is mixing due to convection, the overshooting region located underneath the convectively unstable region is considered part of the convection zone for this calculation.

Obviously, how fast overshooting velocities decay with depth is important for this study, since even velocities much smaller than those inside the linearly convectively unstable region may be able to provide enough mixing so that settling cannot occur. This can have a large effect on the settling rate of heavy elements in a WD surface convection zone, and this in turn has a large effect on the inferred accretion rate of metals such as Mg or Ca. To measure the decay of overshooting, the presented simulations are analyzed statistically. Since the thermal stratification in the overshooting region can be estimated only inaccurately when constructing a starting model the relaxation time is a significant fraction of its associated thermal time scale. The analysis of our pre-calculated 2D simulations showed stable statistical results after a relaxation period of $\approx 100\,\mathrm{scrt}$, where a sound crossing time (scrt) is defined as the traveling time of a sound wave passing the vertical extent of the simulation box. Two dimensional pre-runs as described in [8] have not been performed for the two more recent simulations, since the relaxation period in 2D has to be limited to avoid the mean stratification to drift away from its 3D counterpart. Instead, 3D relaxation from the beginning and, as a faster alternative, 3D relaxation of a model simulated at lower resolution followed by an increase in resolution after initial relaxation have been investigated as alternatives.

2. Governing Equations

The ANTARES (A Numerical Tool for Astrophysical RESearch) code is designed to numerically solve the fluid dynamical equations. Among several options it can do so on an equidistant, three dimensional rectangular grid following the popular box-in-a-star ansatz (see Fig. 2). It can also perform compressible hydrodynamic simulations with radiative transfer in all three spatial dimensions. The source code is written in Fortran90 and parallelized in a hybrid way with MPI and OpenMP, [13]. To avoid high computational costs for global high resolution simulations, a local grid refinement is implemented, too. The order of spatial and temporal discretization can be chosen arbitrarily. However, a 5^{th} order weighted essentially non-oscillatory scheme (WENO5) is favored for the mentioned type of simulations, [9]. This scheme calculates the boundary fluxes of the characteristic variables in their eigenspace and hence guarantees stable up-winding, even at high Mach numbers as they occur in the photosphere of a DA white dwarf. Turbulence is modeled with a Smagorinsky subgrid scale model with a constant of 0.2 and a turbulent Prandtl number of 0.72. The parallel output is realized with HDF5 which is based on MPI. Best parallel performance is expected when each core has to calculate about 200,000 grid points, which typically results in columns of 25×25 points horizontally and, e.g., 320 points vertically. The MPI-decomposition for simulations with radiative transfer is available only horizontally, since the solution process of the radiative transport equation (short characteristics method) cannot be parallelized vertically without massive overhead. The compressible formulation of the problem brings only local boundary communication between the columns, which affects the MPI overhead positively. Hence, no global communication is needed, except for some routines at the beginning of the calculation. The equations governing the dynamics of granulation and convection in the white dwarf stars are as follows:

$$\frac{\partial \rho}{\partial \mathrm{t}} + \nabla \cdot (\rho \vec{u}) = 0, \tag{1}$$

$$\frac{\partial \rho \vec{u}}{\partial \mathrm{t}} + \nabla \cdot (\rho \vec{u}\vec{u} + \mathrm{p}\mathbf{I}) = \nabla \cdot \tau + \rho \mathbf{g}, \tag{2}$$

$$\frac{\partial \rho \mathrm{E}}{\partial \mathrm{t}} + \nabla \cdot (\vec{u}(\mathrm{E} + \mathrm{p})) = \nabla \cdot (\tilde{\mathrm{u}} \cdot \tau) + \rho(\tilde{\mathrm{u}} \cdot \tilde{\mathrm{g}}) + \mathrm{Q}_{\mathrm{rad}}, \tag{3}$$

where, besides standard notation, the total (kinetic + internal) energy is E and the radiative heating and cooling rate is $\mathrm{Q}_{\mathrm{rad}}$. It can be calculated from the radiative energy flux F_ν, [9], according to where an optical depth of 1 is reached. Thus,

$$\mathrm{Q}_{\mathrm{rad}} = -\int_\nu (\nabla \cdot \mathrm{F}_\nu) \mathrm{d}\nu. \tag{4}$$

We are using slip boundary conditions at the bottom and Dirichlet boundaries for the density at the bottom, too. The energy at the radiative lower boundary is fed into the domain by a heat flux $\mathrm{F}_{\mathrm{rad,bottom}} = \sigma \mathrm{T}_{\mathrm{eff}}^4$. The top boundary conditions are open in the sense that fluid can leave and enter the domain but sound- and shock waves are absorbed. This avoids reflecting waves which would heat the fluid locally. The computational time is counted in sound crossing times (scrt), which measures the traveling time of a sound wave, passing the vertical distance. Typical extensions of such a simulation box are $8 - 15\,\mathrm{km}$ horizontally at a height of $6 - 8\,\mathrm{km}$. One scrt is about 0.2 seconds. A meaningful simulation — for statistical post-processing — needs at least 60 scrt in 3D or 12 seconds of physical time, respectively. The numerical time step is limited by the compressible CFL number which is set to 0.25. All three initial 1D stellar model envelopes for the different values of $\mathrm{T}_{\mathrm{eff}}$ are constructed from 1D stellar structure models (see [8] for details). The microphysical properties (equation of state) and input properties for the radiative transfer (opacities) are available as tabulated values (see [9, 8]).

The calculation of the radiative flux needs about 90% of the computational cost. To balance the performance of the entire solver towards the much faster hydro-part, the MPI-boundaries of the radiative flux are communicated from the last stage of the actual time step. This lowers the order of the numerical error, but is stable. Though, this error is small compared to the error obtained by the finite angular resolution. This procedure reduces the MPI overhead significantly and lets the solver scale up to 2048 cores with a scaling efficiency of about 90%. Communicating the latest radiative MPI boundaries stops efficient scaling at 512 cores, depending on the cluster architecture and the MPI domain size. However, the boundary error is only visible at the initialization of the simulations. Here, the MPI communication of F_{rad} may lead to a regular pattern depicting the MPI decomposition. In order to overcome this an adapted initial perturbation routine has been implemented. Now, the perturbation function has the same amount of modes as MPI cores in each direction and acts only in the upper convective zone at the maximum of the super-adiabatic peak. The initial perturbations a simple trigonometric function which is perturbed by a random noise. The noise itself lets the base function fluctuate at most 1%.

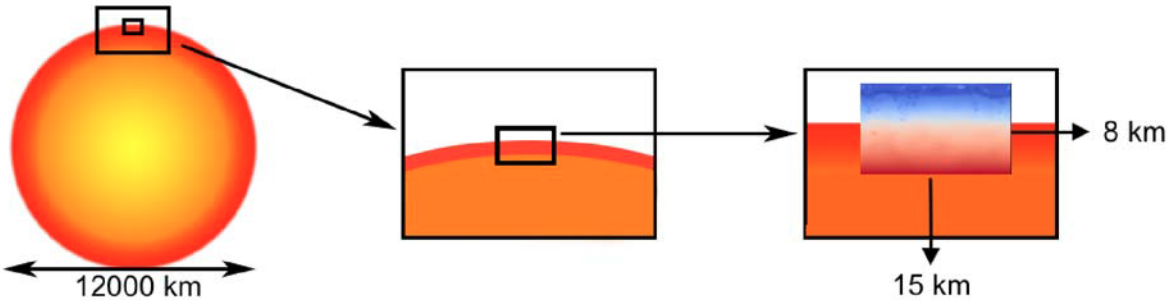

Figure 1. We use the box-in-a-star ansatz available in the ANTARES code suite for the surface convection zone simulation of a hydrogen rich white dwarf (DA). The typical extent of a three dimensional simulation box is 14–15 km. The depth ranges between 7–9 km.

3. Results

The case of $T_{eff} = 11800\,K$ has been investigated in detail in [8]. We here first focus on two more recent simulation runs.

3.1. Case study with $T_{eff} = 12100\,K$

The simulation case with $T_{eff} = 12100\,K$ is calculated in a box with a volume of $8.49 \times 14.2 \times 14.2\,km^3$. Here, the first value is the vertical extension and the following values are the horizontal extension. The maximum temperature at the bottom is $1.2 \cdot 10^5 K$. The grid resolution is set to $211 \times 461 \times 461$ points, respectively. The case was calculated for 63 scrt which corresponds to 16 seconds. Especially, the initial condition has been tested carefully. We found that deep vertical perturbations (> 4 km) lead to long lasting thermal fluctuations which yield to peaks in the radiative flux. It would take significant fractions of the thermal time scale of the simulation box to flatten these peaks (see [7, 8]).

3.2. Case study with $T_{eff} = 12400\,K$

The second case has a resolution of $211 \times 432 \times 432$ points, and a physical domain size of $8.45 \times 14.1 \times 14.1\,km^3$. Except for the bottom temperature and the larger total flux as specified by T_{eff}, and hence the resulting hydrostatic equilibrium stratification, the properties of the

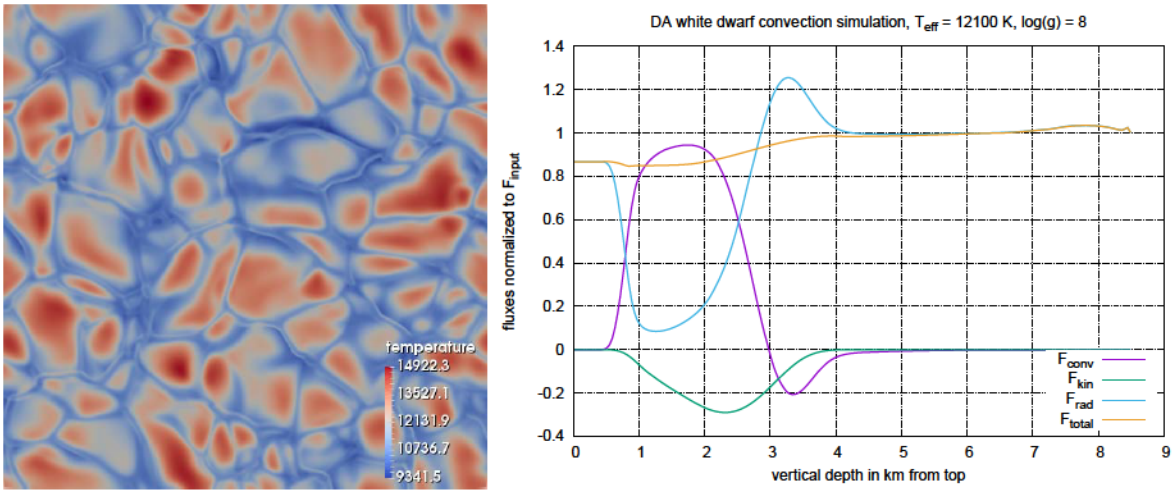

Figure 2. (left) Temperature field for a horizontal slice measured from the top at 520m where the horizontally averaged temperature is $T_{\rm eff} = 12100\,{\rm K}$. (right) Convective, kinetic, radiative and total flux normalized to the input flux $F_{\rm input} = \sigma T_{\rm eff}^4$ at the bottom.

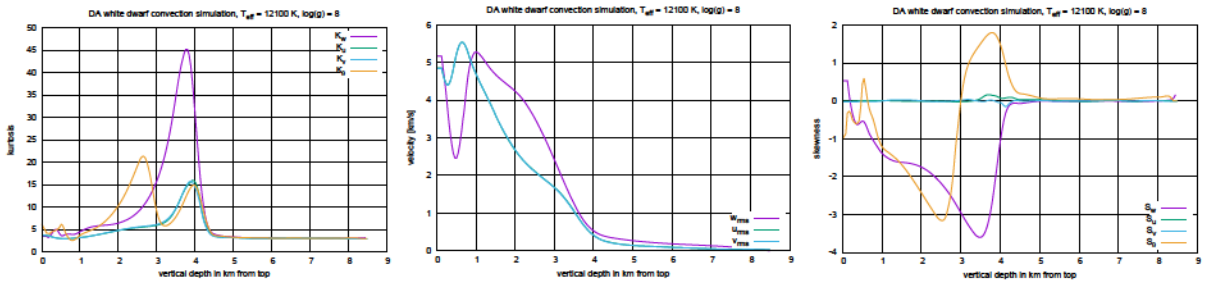

Figure 3. (left) kurtosis, (middle) velocity (rms), (right) skewness for $T_{\rm eff} = 12100\,{\rm K}$

simulation setup are identical to the case $T_{\rm eff} = 12100\,{\rm K}$. However, because the deepest layer, in which $F_{\rm rad}$ notably differs from the total flux, is much closer to the surface for a $T_{\rm eff}$ of 12400 K (compare Fig. 4 with Fig. 2), its associated Kelvin-Helmholtz time scale is also much smaller and indeed, just as explained in [7, 8], thermal relaxation is much faster for this model. Indeed, its total agrees with the input flux to within $\lesssim 2\%$ (see Fig. 4).

4. Conclusion

Comparing root mean square (rms) vertical and horizontal velocities from Fig. 2–5 for the cases of $T_{\rm eff} = 12100\,{\rm K}$ and 12400 K, respectively, with those of Fig. 3 and Fig. 6 to 9 from [8], it becomes clear that the two cooler models are rather similar in terms of convective efficiency, maximum velocity, profile of horizontal and vertical velocity as a function of depth, despite the model with $T_{\rm eff} = 12100\,{\rm K}$ is not yet sufficiently well relaxed. The hottest model with $T_{\rm eff} = 12400\,{\rm K}$ in turn is excellently relaxed. However, the region underneath what is called the wave-dominated region in [8], where $F_{\rm conv} \to 0$ and $F_{\rm rad} \to F_{\rm total} \approx F_{\rm input}$, is distinguished by much higher horizontal velocities than vertical ones. This is the opposite from what is found for the 12100 K and the 11800 K models. We suggest it is related to its lower convective efficiency (and hence lower maximum of $F_{\rm conv}$, as the simulations are all deep with no indications for interaction with the bottom boundary over several pressure scale heights as a function of depth). If we compare the skewness of the different components of the velocity field (vertical

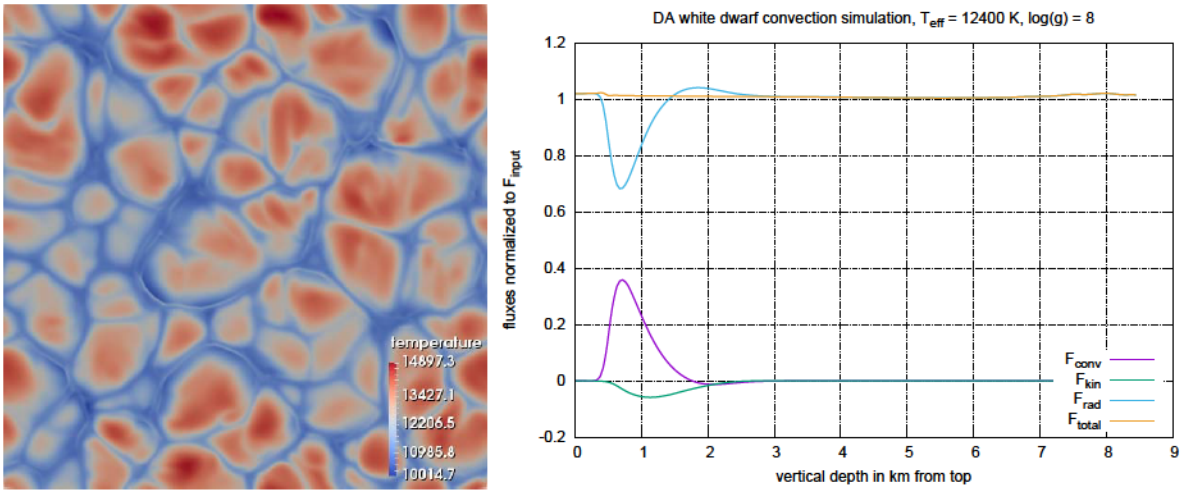

Figure 4. (left) Temperature field for a horizontal slice measured from the top at 520m where the horizontally averaged temperature is $T_{\rm eff} = 12400\,{\rm K}$. (right) Convective, kinetic, radiative and total flux normalized to the input flux $F_{\rm input} = \sigma T_{\rm eff}^4$ at the bottom.

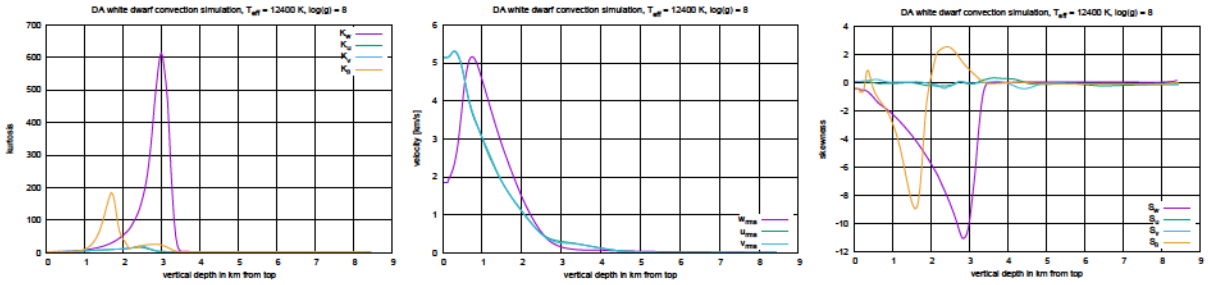

Figure 5. (left) kurtosis, (middle) velocity (rms), (right) skewness for $T_{\rm eff} = 12400\,{\rm K}$

one, w, as well as horizontal ones, u and v) and the temperature field (θ) from Fig. 3 and 5 with Fig. 11 from [8], we again find a close agreement between the two cooler models (with $T_{\rm eff} = 11800\,{\rm K}$ showing the larger absolute values). The hottest model features more extreme absolute values and a drop in S_w without a point of inflection. The same can be concluded for the kurtosis of these fields (Fig. 3 and 5 in this paper and Fig. 12 and 13 from [8]), but for one important difference: for the hottest model the horizontal velocity fields have their maxima much further inside. This has to be related to its smaller convective fluxes and also to the smaller drop in horizontal velocities. Thus, the basic structure of a convectively unstable region on top of a countergradient region, followed by a plume-dominated region where plumes are hotter than their surroundings and the convective flux is negative, and finally a wave-dominated region with essentially zero non-radiative heat flux is the same for all three models. However, the low efficiency (small Peclet number) of the hottest model apparently leads to a different behavior of the horizontal velocities in the wave-dominated region and most likely to differences in the kind of waves being formed there and the mixing efficiency. An extensive comparison with further simulation cases is currently in preparation.

Acknowledgments. FK is grateful for support by the Austrian Science Fund FWF projects P25229 and P29172. MHM gratefully acknowledges support from the United States Department of Energy under grant DE-SC0010623 and the National Science Foundation under grant AST-1312983 and AST-1707419. The simulations were performed mainly at the Northern German

Network for High-Performance Computing (project number bbi00008). Preparation simulations have been performed on the Vienna Scientific Cluster on VSC-2 (project p70708) and the cluster nodes of the Faculty of Mathematics, Univ. of Vienna, on VSC-3.

References

[1] B. Freytag, H.-G. Ludwig, and M. Steffen. Hydrodynamical models of stellar convection. The role of overshoot in DA white dwarfs, A-type stars, and the Sun. *Astron. Astrophys.*, 313:497–516, 1996.

[2] B. Freytag, M. Steffen, H.-G. Ludwig, S. Wedemeyer-Böhm, W. Schaffenberger, and O. Steiner. Simulations of stellar convection with CO5BOLD. *Journal of Computational Physics*, 231:919–959, February 2012.

[3] A. Gianninas, P. Dufour, M. Kilic, W. R. Brown, P. Bergeron, and J. J. Hermes. Precise atmospheric parameters for the shortest-period binary white dwarfs: Gravitational waves, metals, and pulsations. *Astrophys. Jour.*, 794:35, 2014.

[4] H. Grimm-Strele, F. Kupka, B. Löw-Baselli, E. Mundprecht, F. Zaussinger, and P. Schiansky. Realistic simulations of stellar surface convection with ANTARES: I. Boundary conditions and model relaxation. *New Astron.*, 34:278–293, 2015.

[5] D. Koester, B. T. Gänsicke, and J. Farihi. The frequency of planetary debris around young white dwarfs. *Astron. Astrophys.*, 566:A34, 20 pp., 2014.

[6] F. Kupka. Turbulent convection and numerical simulations in solar and stellar astrophysics. In W. Hillebrandt and F. Kupka, editors, *Interdisciplinary Aspects of Turbulence*, volume 756 of *Lecture Notes in Physics*, pages 49–105. Springer, Berlin, 2009.

[7] F. Kupka and H. J. Muthsam. Modelling of stellar convection. *Living Rev. Comput. Astrophys.*, 3:1:159 pp., 2017.

[8] F. Kupka, F. Zaussinger, and M. H. Montgomery. Mixing and overshooting in surface convection zones of da white dwarfs: first results from ANTARES. *Mon. Not. Roy. Astron. Soc.*, 474:4660–4671, 2018.

[9] H.J. Muthsam, F. Kupka, B. Löw-Baselli, C. Obertscheider, M. Langer, and P. Lenz. ANTARES – A Numerical Tool for Astrophysical RESearch with applications to solar granulation. *New Astron.*, 15:460–475, 2010.

[10] P.-E. Tremblay, H.-G. Ludwig, B. Freytag, G. Fontaine, M. Steffen, and P. Brassard. Calibration of the mixing-length theory for convective white dwarf envelopes. *Astrophys. Jour.*, 799:142 (14 pp.), 2015.

[11] P.-E. Tremblay, H.-G. Ludwig, M. Steffen, P. Bergeron, and B. Freytag. Solution to the problem of the surface gravity distribution of cool da white dwarfs from improved 3d model atmospheres. *Astron. Astrophys.*, 531:L19 (5 pp.), 2011.

[12] P.-E. Tremblay, H.-G. Ludwig, M. Steffen, and B. Freytag. Pure-hydrogen 3D model atmospheres of cool white dwarfs. *Astron. Astrophys.*, 552:A13 (13 pp.), 2013.

[13] Zaussinger, F. and Spruit, H. C. Semiconvection: numerical simulations. *Astron. Astrophys.*, 554:A119, 2013.